NOVA
SCIENCE PUBLISHERS, INC.

# THE UPPER MIXED LAYER

Fabrizio D'Ortenzio
Louis Prieur

In: "Life in the Mediterranean Sea: A Look at Habitat Changes"
Editor: Noga Stambler
ISBN: 978-1-61209-644-5 2012

400 Oser Avenue, Suite 1600
Hauppauge, N. Y. 11788-3619
Phone (631) 231-7269
Fax (631) 231-8175
E-mail: Main@novapublishers.com
http://www.novapublishers.com

In: Life in the Mediterranean Sea: A Look at Habitat Changes ISBN: 978-1-61209-644-5
Editor: Noga Stambler 

***Chapter 5***

# THE UPPER MIXED LAYER

***Fabrizio D'Ortenzio and Louis Prieur***
CNRS and University P. & M. Curie, Laboratoire d'Océanographie de Villefranche, Villefranche-sur-mer, France

## 1. ABSTRACT

Compared to the global ocean, the upper ocean mixed layer in the Mediterranean Sea shows specific and peculiar characteristics. Available climatological observations, describing the large and seasonal scales of the Mediterranean upper mixed layer, indicate strong east-west gradients and a temperate sea seasonal cycle. The first is induced by the surface circulation of the basin, which is mainly composed of the eastward flow of Atlantic water, forced by the thermohaline Mediterranean cell. The second is generated by the atmospheric mass flux cycling, which is the main forcing term of the Mediterranean mixed layer.

The dynamics of the forcing terms at small scales (i.e. hourly or 1 km) is, however, particularly relevant in the Mediterranean, mainly because of the limited size of the basin. Based on a few selected observational examples, we highlighted that the small scales of forcing factors significantly contribute to Mediterranean mixed layer dynamics, and, in some cases, they should explain most of the observed variability. Observations of these scales are, however, scarce, and the definitive characterization of their impact on the Mediterranean mixed layer is still far from complete.

Particular attention is devoted to wind stress. In the Mediterranean, due to the specific coastal and continental orography configuration, the wind regime impacts in several ways on the mixed layer dynamic. It plays a role in large-scale circulation, in the generation of sub-basin permanent oceanic structures and in local density oceanic field modification. All these processes control the Mediterranean mixed layer dynamics, and cannot be neglected if a correct determination of upper ocean dynamics is required.

## 2. INTRODUCTION

The marine trophic chain begins in the upper layers of the ocean. In the region located just below the interface between the atmosphere and the ocean, the first element of the trophic

chain, phytoplankton, finds all the elements required for growth. Consequently, secondary producers (i.e. zooplankton), as well as bacteria and viruses, spend most of their lifetime in this layer.

Favorable conditions for phytoplankton growth occur when light and nutrients are available (for a complete review see Mann and Lazier, 1996 and reference therein). The solar light, which propagates through the almost transparent atmosphere, is rapidly attenuated by seawater in the visible portion of the spectrum; solar energy, required by phytoplankton for the photosynthetic processes, is consequently more elevated at the surface than at depth. In the surface layers, however, nutrient concentrations are generally low (Longhurst, 1995), and rapidly consumed by phytoplankton. Consequently, in a generally stratified ocean, nutrients are mainly concentrated below illuminated depths, where excretion and losses accumulate, and are re-mineralized by viruses and bacteria. Only when vertical exchanges occur, important nutrient concentrations are injected in the surface layer, and can be used by phytoplankton.

The availability of nutrients in surface layers is then primarily driven by the mixing of the water column (see Williams and Follows, 2003 for a complete review). The mixing is particularly strong in the upper layers of the ocean, where permanent energy exchanges (mechanic and thermal) occur with the adjacent atmosphere. If energy is sufficiently high, the mixing of the upper layers will induce a uniform density layer, i.e. the upper mixed layer.

Although relatively simple, this definition hides the complexity of the process driving the mixed layer set up, which is generally complicated by several energetic sources (i.e. oceanic advection, turbulence, current shear). Moreover, all these processes act on the upper layer density field at different spatial and temporal scales, which spawn from mesoscale to basin spatial scale and from diurnal to interannual temporal scales. Consequently, the mixed layer is generally defined in operational ways, using empirical criteria on in situ profiles (Kara et al. 2000, de Boyer Montegut et al. 2004, D'Ortenzio et al. 2005).

In spite of its limited size (~ 0.6% of the global ocean surface, 0.3% of its volume), the Mediterranean Sea is considered one of the most complex marine environments on Earth (Williams, 1998). The Mediterranean Sea is a semi-enclosed basin connected with the Atlantic, via the Gibraltar strait, and with the Black Sea, via the Dardanelles Strait. It is divided in two main sub-basins, Eastern and Western Mediterranean (EMED and WMED hereafter) by the strait of Sicily (about 400 m depth).

The Mediterranean is a concentration basin, where the evaporation exceeds the sum of precipitation and river runoff input (Hopkins, 1985). The long-term equilibrium of both water and salt budgets brings an outflow across the strait of Gibraltar ranging from 0.8 to 1.6 Sv (Bethoux, 1979; Hopkins, 1999, Ribera d'Alcalà et al. 2003).

Two main, distinct, thermohaline cells drive the large scale circulation: the WMED cell, forced by deep water convection events in the northwestern Mediterranean, and the EMED cell, driven by deep water formed in the Adriatic Sea. Because of the shallow sills at the Gibraltar and Sicily straits, significant exchanges between the two sub-basins and with the Atlantic involve mostly the intermediate layers (Astraldi, et al., 1999). An intermediate circulation is present, primarily forced by intermediate (300-500m) waters (LIW) formed in the Levantine basin, which spread westward, to finally flow into the Atlantic (see Robinson et al. 2001 for a detailed description of the Mediterranean deep and intermediate circulations).

The seasonal cycling of the Mediterranean mixed layer is, at first order, controlled by atmospheric forcing (heat fluxes and wind stress). Heat flux regime, typical of temperate seas,

is composed by an intense warming in summer and by a relative cooling during winter, which could be reinforced, in specific areas of the basin, by wind forcing (see for example Castellari et al. 1998). The Mediterranean mixed layer seasonal cycling mimics the above evolution, with a relatively slow deepening and cooling in winter and an abrupt shallowing in summer (D'Ortenzio et al. 2005).

Mediterranean mixed layer waters are primarily composed by waters of Atlantic origin (AW), which, entering through the Gibraltar Strait, flow eastward following the inverse estuarine circulation driven by deep and intermediate thermohaline cells. In its eastward flow, AW progressively loses buoyancy and, under the influence of wind stress (Malanotte-Rizzoli and Bergamasco, 1989, 1991, Molcard et al. 2002), produces meanders and jets, which in fact alter the density structure of upper layers. In addition, AW interacts with sub-surface and intermediate waters, progressively increasing both temperature and salinity.

A complex and intricate set of sub-basin structures (100-300 km length scale) is observed (Pascual et al. 2007, Hamad et al. 2006), mainly induced by the interactions between AW spreading, complex basin topography and wind stress curl. Permanent and recurrent features with cyclonic (Gulf of Lions, Northern Tyrrhenian, South Adriatic, Rhodes) and anticyclonic (Alboran, Ierapetra, Cyclops, Shikomona) regimes are present and contribute to modify surface water characteristics and, consequently, mixed layer dynamics.

Consequently, the dynamics of the upper mixed layer in the Mediterranean Sea is extremely complex and is the result of the interactions among atmospheric forcing, large-scale circulation, sub-basin and mesoscale activities, and topography influence. All these processes affect the basin upper layers at several, and often interconnected, temporal and spatial scales.

For all these reasons, the dynamics of the Mediterranean upper mixed layer is still not entirely defined. Observations are available, as the Mediterranean was intensively sampled in the last decades, but they are still not sufficient to cover all the scales involved (in particular the smallest ones). A climatological analysis was, however, realized (D'Ortenzio et al. 2005) and it constitutes the most important source of information presently available on the Mediterranean upper mixed layer at basin. An intense modeling effort is also dedicated to the representation of Mediterranean physical dynamics (among others Sannino et al. 2009, Tonani et al. 2008, Fernandez et al. 2005, Béranger et al. 2005). However, Mediterranean models are more focused on the general circulation of the basin and very few studies exist focusing on mixed layer dynamics (i.e. Lascaratos et al. 1993).

The main consequence of the imperfect characterization of the upper layers in the Mediterranean Sea is that the impact of the mixed layer evolution on Mediterranean ecosystems is not well understood, although it is one of the key points for physical biological interaction studies in the marine environment (Sverdrup,1953; Riley, 1946).

In this chapter, we will present an overview of the behavior of the Mediterranean upper mixed layer and its forcing factors, with a particular emphasis on atmospheric forcing. The different spatial and temporal scales of the main processes affecting mixed layer dynamics will be discussed, giving examples based on the available observations and deliberately overlooking modeling results.

# 3. THE MEDITERRANEAN MIXED LAYER

## 3.1. Generalities

Most of the time, the ocean is stratified. The cold and dense waters are located at depth, whereas surface layer waters are warm and less dense. Water density, then, increases constantly with depth. However, in the layer just below the ocean-atmosphere interface, water characteristics are constant and almost homogeneous. The thickness of this layer is defined as the mixed layer depth.

The mixed layer is, then, the oceanic boundary layer between atmosphere and ocean, where exchanges of heat, water, and momentum with the atmosphere and deep ocean layers occur. Consequently, the ocean receives or loses energy through the mixed layer.

If $h$ is the mixed layer depth, and $Q$ is heat, salt (water), momentum or buoyancy, the content of $Q$ in the mixed layer can be expressed, at each instant $t$, as $h<Q>$, where $<Q>$ indicates the average value of $Q$ between the surface (0 m) and the mixed layer depth ($h$).

The temporal variations of the content $h<Q>$ can be expressed in a simplified form as:

$$\partial( h<Q>)/\partial t = J_Q + Q_i \quad (1)$$

where $J_Q$ is the net surface flux of $Q$ between the atmosphere and the ocean at time $t$, and $Q_i$ indicates all the other possible sources modifying the water column content from the surface to depth $h$ (i.e. vertical and horizontal advections of $Q$ or absorption of solar energy by water and phytoplankton).

Equation (1) formalizes the effects of air-sea exchanges on the temporal evolution of $<Q>$ and consequently of $h$, allowing a formal approach to determine it[1].

To indicate the stability of a water parcel, we will refer to buoyancy, which is defined as the $-g\rho$, where $g$ is the gravitational acceleration and $\rho$ is the water parcel's density. Buoyancy is also often reported as an acceleration (m $s^{-2}$) and defined as $g(\rho_0-\rho)/\rho_0$, where $\rho_0$ is a reference density value, defined to have a correspondent upward acceleration.

If we consider equation (1) for buoyancy, the term $J_b$ should summarize all the factors modifying mixed layer buoyancy through the air-sea interface. It can then be expressed as (Gill, 1982):

$$J_b = g\,\alpha\,Q_{net}/(\rho_s\,C_p) + g\,SSS\,\beta\,Q_e/(\rho_s\,L_v) \quad (2)$$

where $J_b$ is the buoyancy flux (in $m^2 s^{-3}$) from the atmosphere to the ocean, $Q_{net}$ and $Q_e$ are respectively the net heat and water fluxes modifying salinity (in W/$m^2$), $\rho_s$ is surface water

[1] A complete formulation of the equation 1, showing the complete eulerian $Q$ budget of oceanic mixed layer, can be found in Niiler and Krauss (1977), Gaspar et al. (1990), or Caniaux et al. (2005). The formulation presented here does not explicitly develop the $Q_i$ term, neglecting the vertical integration of the horizontal advection and the vertical advection at the basis of mixed layer. Because we mainly focus on the relationship between surface fluxes and the mixed layer content, the $Q_i$ term is considered a secondary term. Note, however, that equation 1 is not sufficient to determine $h$ and $<Q>$. In mixed layer modeling, other equations, such as the continuity and kinetic budget equations (accounting for the vertical stability of the $h$ column above the stratified ocean, the heat and water exchanges with atmosphere at the surface and the mechanical energy inputs from the atmosphere through the surface wind stress) should be solved to evaluate $h$ and $<Q>$.

density, $SSS$ is sea surface salinity, $C_p$ and $L_v$ are specific heat capacity and latent heat coefficients and $g$ is the gravity acceleration. The terms $\alpha$ and $\beta$ are the thermal and the salinity expansion coefficients for seawater, and are represented by:

$$\alpha = - (1/\rho_s)\, \partial\rho_s/\partial SST \tag{3a}$$

$$\beta = (1/\rho_s)\, \partial\rho_s/\partial SSS \tag{3b}$$

where $SST$ is the sea surface temperature (°C).

From equation (2), the mass flux, $J_m$ (kg/m$^2$s), can be obtained by simply multiplying $J_b$ by a factor indicating the water mass to be modified, which is, in our case, the entire mixed layer:

$$J_m = - J_b\, \rho_s/g \tag{4}$$

Note the opposite sign of $J_m$ and $J_b$, which formalizes the convention of positive mass flux (i.e. water density increase) when the buoyancy flux is negative (i.e. buoyancy decrease), and *vice versa*.

Equations 2-4 indicate that any variation in atmospheric terms ($Q_e$ and $Q_{net}$ in equation 2) induces modification of the buoyancy flux, which, in turn, can generate variations in mixed layer depth ($h$ in equation 1). To explain the impact of $J_m$ on the upper ocean, additional processes should, however, be considered.

1) Without any wind stress and with a hypothetic weak water thermal capacity $Cp$, heating should start approximately at winter solstice, while cooling at the summer solstice. However, water $Cp$ is high and induces a temporal delay in ocean heating and cooling.
2) Most of the time, the upper layers of temperate seas are gravitationally stable (cold layers are deeper than warm layers). When the ocean is heated from above, a new, thin and warmer mixed layer is rapidly formed (i.e. few hours) at the surface. Conversely, when the ocean surface is cooled, the entire existing mixed layer has to be cooled, to create a change in temperature. In addition, as surface cooling induces a density increase in waters close to the surface, the mixed layer becomes gravitationally unstable. To re-equilibrate the vertical density field, convection occurs and mixed layer depth increases (Niiler and Krauss, 1977, Woods and Barkman, 1986). The convective process, then, induces a mixing of surface and underlying waters, which, in turn, mix the temperatures of the involved layers.

In other words, the deepening of the mixed layer is slowed by the temporal scales of convective processes (i.e. few hours or days) and by the relevant quantity of water mass that needs to be modified. The two processes, shoaling/warming and deepening/cooling of $h$/$SST$, have different characteristic time scales. When $J_m$ is negative, $h$ retreats, and, consequently, $SST$ variations are stronger and faster than when $J_m$ is positive and $h$ deepens.

The other main atmospheric forcing term, the wind, is implicitly considered in equations 2-4, by influencing $Q_e$ and $Q_{net}$ in equation (2), and by modifying the oceanic density field

($\rho_s$), through Ekman pumping and shear instabilities (Pond and Pickard, 1983). Finally, the buoyancy flux (and consequently the mixed layer depth $h$) is strictly dependent on the advective (i.e. the vertical or horizontal transport of water) and diffusive processes, which are dependent on the local density field ($\rho_s$ in equation 2).

For the specific case of the Mediterranean Sea, atmospheric forcing variability and its interactions with the Mediterranean surface density field have already been described at different scales (see for example Castellari et al. 1998 and Korres et al. 2000, and reference therein). However, less attention has been given to the multi-scale effects of the ensemble of forcing factors on mixed layer dynamics of the basin.

To elucidate this point, we will describe some examples, based on data, of buoyancy flux variability (as a proxy of the atmospheric forcing), addressing separately spatial and temporal scales. The main aim here will be to highlight which scales should be considered relevant in the Mediterranean Sea and why. After that, when the scales of the forcing factors have been identified, we will try to furnish experimental examples of their effects on Mediterranean basin mixed layer dynamics.

## 3.2. The Temporal Scales of the Mediterranean Atmospheric Forcing

The temporal evolution of the $J_m$ term (as defined by equation 4) is characterized by several intricate and interconnected temporal scales, related to the circulation of air masses crossing the study area (Lionello et al. 2006a and references therein).

An illustrative example of the $J_m$ multi-scale temporal evolution in the Mediterranean Sea is shown in Figure 1. $J_m$ is derived using $Q_{net}$ and $Q_e$ (see equation 2) products from the European Centre for Medium-range Weather Forecast (ECMWF) operational model (T213/L31 model version at 0.5° spatial resolution and with a 4D-VAR assimilation system in a 6 hour cycling, Rabier et al., 1998). Data have six-hour temporal resolution and were extracted from years 2004 to 2008 in a point located at 8°E and 43°30'N (northwestern Mediterranean Sea)[2].

The time series of $J_m$ (kg/m$^2$s, grey line, central panel, Figure 1) was temporally filtered with a 1-day moving box (thick black line) and the time-cumulated $J_m$ was calculated (thin black line, central panel) and temporally de-trended[3]. Additionally, wind stress (ECMWF product, lower panel, N/m$^2$) and $SST$ (ECMWF product, upper panel, °C), with its temporal first derivative computed with a $\Delta t$=10 days, were also depicted. $SST$ was selected here as an example of an oceanic parameter which can be perturbed when mixed layer modifications occur.

[2] The point has been selected as it could be representative of the mean North Western Mediterranean forcing, but also because is the site of the only available long term station of in situ and atmospheric observations (DYFAMED/BOUSSOLE station, Marty, 2002 and Antoine et al. 2006, and ODAS meteorological buoy, www.meteo.shom.fr/real-titme/html/dyfamed.html).

[3] The Mediterranean basin loses water (about 1m/year, mainly for evaporation), which is compensated by the inflow of AW (Mariotti et al, 2002). The compensation effect is not considered in our mass flux computation, resulting in a cumulated mass flux, which increases linearly from one year to another. Because evaporation and AW inflow are relatively constant, or slightly variable, they could reasonably be considered as linearly increasing. Therefore, to simplify, we plotted cumulative detrended mass flux for one day arbitrarily around +6 kg/m$^2$ value on Y-axis. Additionally, the cumulated detrended mass flux is divided by 20 to clarify the plot.

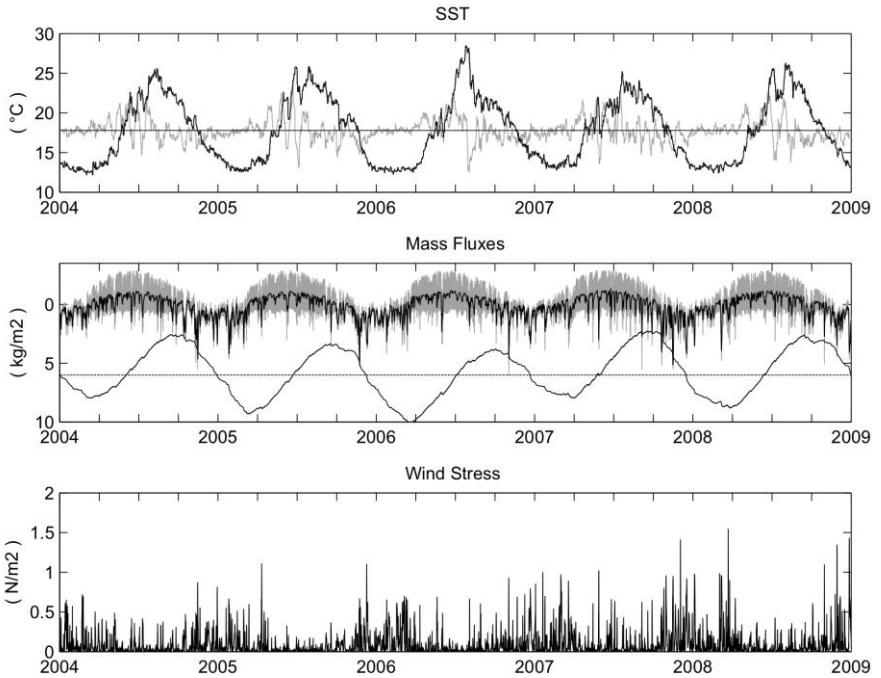


Figure 1.Time series of ECMWF atmospheric and oceanic variables in the northwestern Mediterranean Sea (8°E, 43.5°N) for the period 2004-2008. Upper panel: Sea Surface Temperature, $SST$ (°C, black line) and its first derivative (°C/10 days, grey line). Central Panel: 6 hour mass flux, $J_m$(kg/m$^2$/s, grey line, multiplied by 86400s for plot clarity); daily mass flux, $J_m$ (kg/m$^2$/s, black line, calculated filtering with a $\Delta t$=24 hours); cumulated mass flux (detrended, thin black line, see note 3, divided by 20 for plot clarity). Lower panel: wind stress (N/m$^2$). Note that the y-axis for the central panel is in reverse order to facilitate comparison with $SST$ (upper panel). On the x-axis, ticks indicate solstices and equinoxes.

Four temporal scales are evident in the selected example: interannual, annual, diurnal and chaotic scales.

At annual and diurnal scales, mass flux evolution is prevalently cyclical, indicating that, at these scales, solar forcing is the main driver of $J_m$.

The annual cycle is more evident when the filtered evolution is analyzed. Characterized by annual minima at the summer solstice (about -3 kg/m$^2$ per day) and by maxima at the winter solstice (with weak positive values, blurred by peak influence), the annual variability of $J_m$ is synchronous with the solar radiation cycle. Consequently, the amplitude of the $J_m$ annual cycle varies during the year, depending upon the meridian solar elevation at noon, which is, in turn, dependent on latitude.

Similarly, the $J_m$ diurnal cycle is dependent on solar radiation and daylight duration. Although hard to identify in Figure 1 (the diurnal cycle is poorly resolved graphically and the decreasing and increasing daily mass flux variations are too closely juxtaposed). Evidence of the diurnal cycle scale is obtained when the filtered and unfiltered mass flux trends are compared (black and grey lines in Figure 1, central panel). Daily cycle amplitudes (grey line) are maximal in summer and, importantly, they are often higher than the corresponding year's filtered mass flux amplitudes (black line). In other words, the exchanges between the atmosphere and the ocean during a day and during a season have comparable strength.

The detrended cumulated mass flux (black thin line in Figure 1, central panel) smoothes all peaks, highlighting the interannual variability of atmospheric forcing, but also its cyclical behavior. Annual maxima (minima) are always observed in spring (autumn), close to equinoxes, as expected, considering seasonality in daylight duration (note that Y-axis is reversed).

Superimposed on the sun-driven annual and diurnal cycles, a chaotic succession of high frequency pulses is observed in the $J_m$ evolution. They are generated by wind stress, which, at Mediterranean latitudes, generally acts with pulses of variable temporal duration (see lower panel, Figure 1), directly and rapidly influencing $J_m$ (via the $Q_{net}$ and $Q_e$ terms in equation 2). In the Mediterranean example (Figure 1, compare lower and central panels), at each wind stress peak (> 0.1 N/m$^2$, or $U_{10}$ wind about 10 m/s) corresponds clearly to a mass flux increase.

The annual mixed layer depth and $J_m$ maxima and minima, as well as the "shape" of their annual evolution, should be similar, with maxima observed not far from equinoxes. As mixed layer observations were not available on the selected site at the required temporal scales, *SST* evolution was analyzed instead, as it could help to address the effect of $J_m$ forcing on the mixed layer. In fact, any $J_m$-induced mixed layer modification should have a similar (though opposite) variation on *SST*.

In the shown example, the *SST* annual cycle is not symmetric. During winter, minima are close to 13°C and quite constant for most of winter, and even high mass flux values induce weak SST modifications. Likely, the mixed layer was deep (>100 m) and at depth temperature was close to *SST*. Conversely, summer *SST* is more peaked, with an evident interannual variability of the annual maxima values (spreading from 24° and 28°C) and timing, which likely coincides with mixed layer depth minima. Interannual variability is also evident in the temporal duration of winter *SST* minima (less than 2 months in 2005 and more than 4 months in 2008). In our example, then, we confirmed the discrepancy between the $J_m$ and *SST*/Mixed layer depth time evolutions: the former could be properly approximated by a sinusoidal function, while not the latter.

All of the above is, however, modulated by wind stress, as mild winds facilitate warming, although strong winds increase mixing. In our example, during July 2006, maximum *SST* values were observed after about 1 month of weak winds.

To summarize, four scales characterized the $J_m$ variability and modulate the *SST* and *h* cycles in our Mediterranean example:

1) an annual/seasonal scale, which induces the yearly stratification/destratification cycles and the seasonal mixed layer depth *h* and *SST* variations; it is characterized by a well-marked annual cycle, which exhibits summer maxima and winter minima and it is forced by the solar cycle; however, the $J_m$ and *SST*/*h* cycles are not phased, although the first is the main forcing factor of the second two.
2) a daily scale, which modulates the mean seasonal variability and induces diurnal *h* and SST cycling, more evident in summer than in winter, as appreciable only when *h* is shallow. Noticeably, as the daily $J_m$ variability is comparable to the $J_m$ annual cycle, neglecting daily scales could compromise the assessment of the mixed layer depth evolution.
3) a chaotic/high frequency scale, induced by wind, which generates strong perturbations of the former two cycles; the wind effect is season-dependent: in

winter, strong winds have relevant impact on the mixed layer depth, although a very weak effect on the *SST*; in summer, the opposite is observed. Moreover, the high frequency scale induced by the wind generates important mesoscale features on the ocean, which largely affect the local mixed layer (Molcard et al., 2002, Malanotte-Rizzoli and Bergamasco, 1991, Horton et al., 1994).

4) an interannual variability, which impacts all the previous scales and is related to the atmospheric circulation of the middle latitudes, although its intensity is relatively weak (but see later).

## 3.3. The Spatial Scales of the Mediterranean Atmospheric Forcing

In the Mediterranean area, the mass fluxes and wind stress spatial variations are mainly driven by the size of the air masses (about 1000 km) crossing the region (Lionello et al. 2006b and references therein). Mediterranean cyclones last one week, on average, in the basin area and are more intense in winter than in summer. Finally, the wind regime is influenced by some recurrent and constant winds (i.e. Mistral, Tramontana, Sirocco, Etesian, Bora, Khamsin, Sharv), which occur in the northern part of the basin, and which modulate the wind dynamics associated to the atmospheric perturbations.

Once more, we prefer to show some examples of spatial variability of the atmospheric forcing factors rather than discuss the Mediterranean meteorological regimes in detail where extensive literature already exists (for more details see, for example, Ruiz et al. 2008 or Matsoukas et al. 2007 for heat budget and Zecchetto and Cappa, 2001, for wind).

From the ECMWF data set (see previous paragraph), data were extracted at some grid points located in five regions of the Mediterranean: the Gulf of Lions, the Algerian and Ligurian seas for the WMED and the Ionian and Levantine seas for the EMED. Cumulated mass fluxes were calculated (see paragraph 3.1) and the interannual linear trend was removed from the resulting time series (see notes 3 on paragraph 3.2).

At the different Mediterranean locations, (Figure 2) $J_m$ exhibits the general pattern sketched out in the previous paragraph, characterized by positive values in winter (flux from ocean to atmosphere) and negative values during summer (from atmosphere to the ocean). The main dissimilarities among the regions were observed in the difference between the annual maxima and minima. In some years (i.e. 2005), the difference could be important: about 140 kg/m$^2$ between the two extremes, represented by the Gulf of Lions and by the Levantine time series. The mean annual values remain, however, very close.

The western regions appear more variable: the Algerian region shows the greater negative values, while, the Gulf of Lions and the Ligurian areas exhibit the largest positive values. Conversely, in EMED, the time series are smoother and the differences between summer and winter less pronounced. The timing of the positive and negative annual peaks also differs among the regions. Maxima are generally near to the equinoxes, although they are closer to equinoxes in the WMED than in the EMED. The maxima values in the EMED are observed a few weeks before the equinoxes.

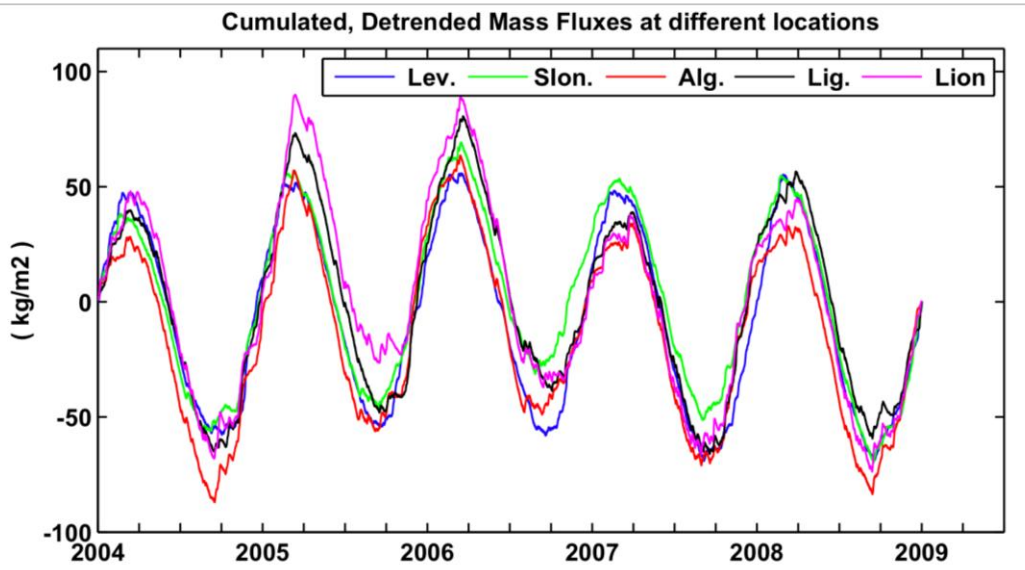


Figure 2. Time series of detrended cumulated mass flux at different Mediterranean locations; *Lev*: Levantine Sea; *Slon*: South Ionian Sea; *Alg*: Mid Algerian Basin; *Lion*: Gulf of Lions offshore; *Lig*: Ligurian Sea central part.

Generally, the winter-to-summer difference is more pronounced in the Western than in the Eastern basin. The observed differences could directly affect the annual mixed layer variability, which we guess will mimic the observed spatial variability of the mass flux. As the mass flux is the primary upper ocean forcing factor (cfr. previous paragraph), we expect, then, to observe similar effects also in the mixed layer spatial pattern.

However, the impact of atmospheric forcing on the upper water column is also depending on surface layer water characteristics (see Generalities). Advective processes could modify these characteristics and then induce a variability of the mixed layers, which results disconnected from the atmospheric forcing. In the Mediterranean, where surface circulation is strongly advective (see Introduction), this point could be crucial and will be discussed in the next paragraph.

## 3.4. The Surface Salinity Field

In the Mediterranean Sea, the oceanic density field is driven by variations in salinity and influenced by the specific orography of the basin (inflow at Gibraltar, evaporation and precipitation regimes, rivers). Climatologically, the winter salinity distribution (MEDAR, 2002, Figure 3) is characterized by an important east-west gradient, with the lowest values in the southwestern surface waters (Figure 3, upper panel). Surface salinity progressively increases in the northern and central regions of the WMED and exhibits the basin maxima in the easternmost region of the Mediterranean (the Levantine area). At deeper layers (150 m, Figure 3, lower panel), salinity is much more homogenous, although an east-west gradient is still observed.

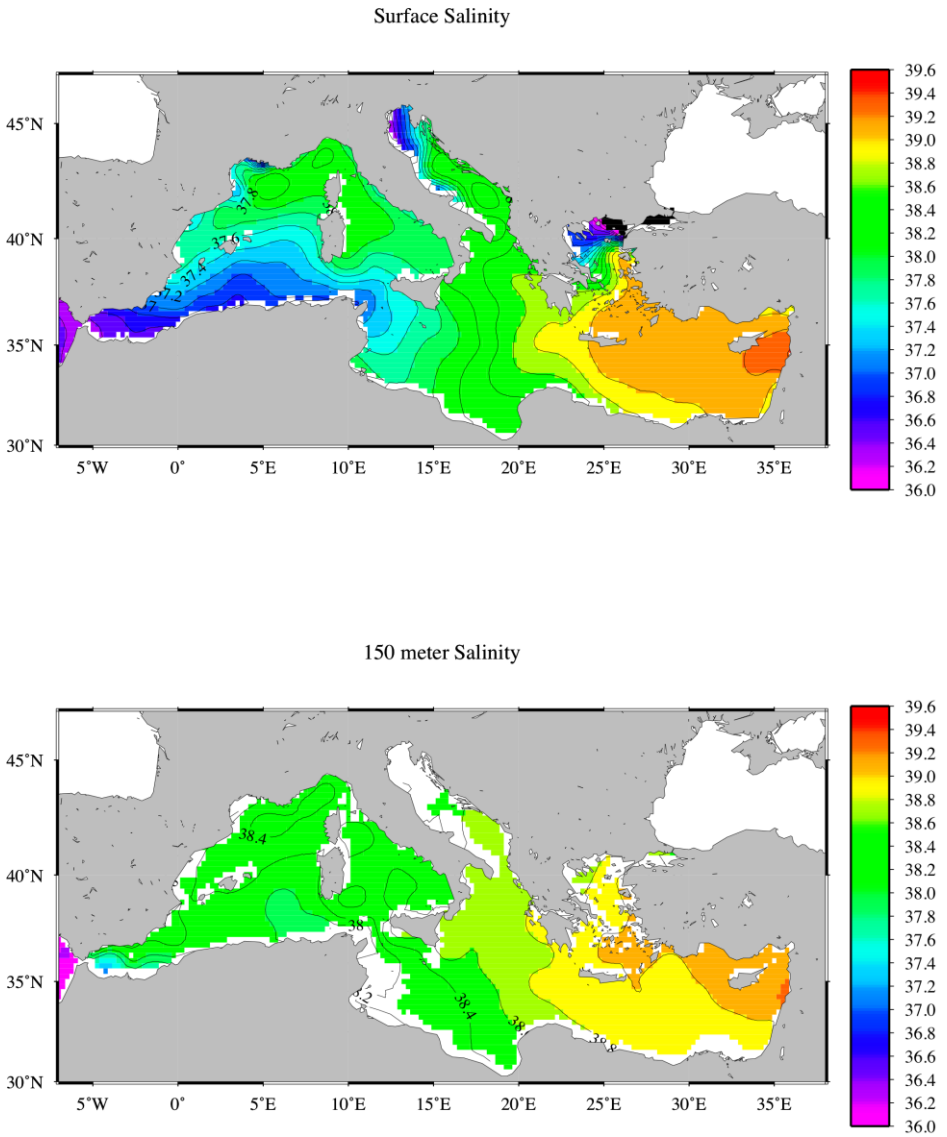


Figure 3. Climatological salinity field (from Medar/Medatlas data base, MEDAR, 2002): surface (upper panel) and 150 m (lower panel).

The surface salinity distribution is mainly induced by the flow of AW, which, penetrating progressively in the basin from Gibraltar, modifies its salinity under the influence of evaporation and mixing with existing underlying Mediterranean waters. The main feature of the AW flow is the existence of a strong (36.5 to 38, compare upper and lower panels in Figure 3) and deep (about 100 m) halocline in the Alboran Sea, just east of Gibraltar. Moving northward and eastward, the halocline progressively attenuates and disappears for longitude greater than 22°E, where the vertical gradient is inverse (compare again upper and lower panels of Figure 3). The main consequence of the observed salinity gradient is a strong and permanent pycnocline, which reflects salinity spatial distribution and which is mainly generated by AW advection and spreading. We can postulate, then, that the Mediterranean

mixed layer depth spatial distribution should be strongly influenced by the AW layers. In fact, the stronger the AW-induced pycnocline, the more intense the atmospheric forcing should be, to break the upper stratification and change the mixed layer, and vice versa. Refer to Figure 3:

1) in the southwestern regions of the basin (Alboran Sea, Algerian basin, South Ionian), where the effect of the AW is larger, the density vertical gradient is particularly intense, which likely avoids any penetration of the mixed layer at depths greater than the AW layer (about 100-150m, Hopkins, 1985).
2) in the EMED, the vertical density gradient is weak, as the depth of the AW layer is reduced by the interactions with the atmosphere and with the existing Mediterranean waters; breaking atmospherically the stratification in these regions could then be relatively easy and, consequently, the mixed layer should be relatively deep;
3) in the northern regions of the basin (Ligurian Sea, Adriatic Sea, Aegean Sea), the intensity of the permanent halocline is also reduced, as the overall cyclonic circulation of the basin (Millot and Taupier-Letage, 2005) advectes AW, which was already strongly modified (more dense in surface, then more close to deep values) during its Mediterranean path (some authors referred to MAW, Modified Atlantic Water, Malanotte-Rizzoli et al. 1997). Consequently, mixed layer depth in the north of the basin is expected to be greater than in the south.

To summarize, the spread of the AW induces important characteristics of the Mediterranean upper circulation, which is supposed to greatly influence the mixed layer dynamics of the basin. Other advective processes, such as frontal systems or coastal water injections, could generate similar effects, though they are hard to detect in a climatological analysis (see e.g. North Adriatic surface salinity anomaly). This point concerns, in fact, all the mechanisms listed until now, as available mixed layer observations in the Mediterranean do not cover all the scales involved. In the following, we will review the existing data and check whether these data confirm our previous description of Mediterranean mixed layer dynamics.

## 4. THE MEDITERRANEAN MIXED LAYER: THE OBSERVATIONS

Generally, the mixed layer depth ($h$) is considered a good proxy of mixed layer dynamics and several methods were proposed to estimate $h$ from in situ data (see appendix for a review). However, not all scales could be addressed and described, as the chronicle observation scarcity limits our estimation at some specific scales.

In the Mediterranean Sea, only the seasonal and sub-basin scales should be analyzed in detail, as a monthly 0.5° climatology was proposed at these scales by D'Ortenzio et al. (2005). At smaller scales, data scarcity becomes more critical and the evaluation of mixed layer dynamics is hard to achieve. Therefore, in the following, we selected two specific examples, both based on observations collected in the northwestern region of the basin, at the long-term station DYFAMED/BOUSSOLE (8°E, 43.5°N, Marty et al. 2002, Antoine et al. 2006). They will be analyzed to evaluate the mixed layer dynamics at small scales and to identify its interplay with the forcing factors.

## 4.1. The Basin Scale, Seasonal Dynamic of Mediterranean Mixed Layer

The climatology proposed by D'Ortenzio et al. (2005) was based on more than 250,000 temperature profiles collected in the Mediterranean Sea from 1980 to 2002, and it consists of monthly mixed layer depth maps, calculated with a 0.5 °C temperature threshold method (see appendix). Mixed layer depth estimations calculated on single profiles were averaged on a 0.5° mesh box, and the intra-box standard deviation was also computed.

Mean seasonal evolution, the calculated averaging of the climatological fields over different regions of the basin (Figure 4, upper panel), confirmed that the mixed layer depth seasonal cycle in Mediterranean Sea is primarily driven by mass fluxes. In winter, mixed layer depths are deep, with maxima between 50 and 70m, observed during January/February, for both WMED and EMED. Abrupt retreat occurs in spring (30-40 m during April), whereas very narrow mixed layers are observed during summer (lower than 20 m). From September, mixed layer depths begin to deepen again.

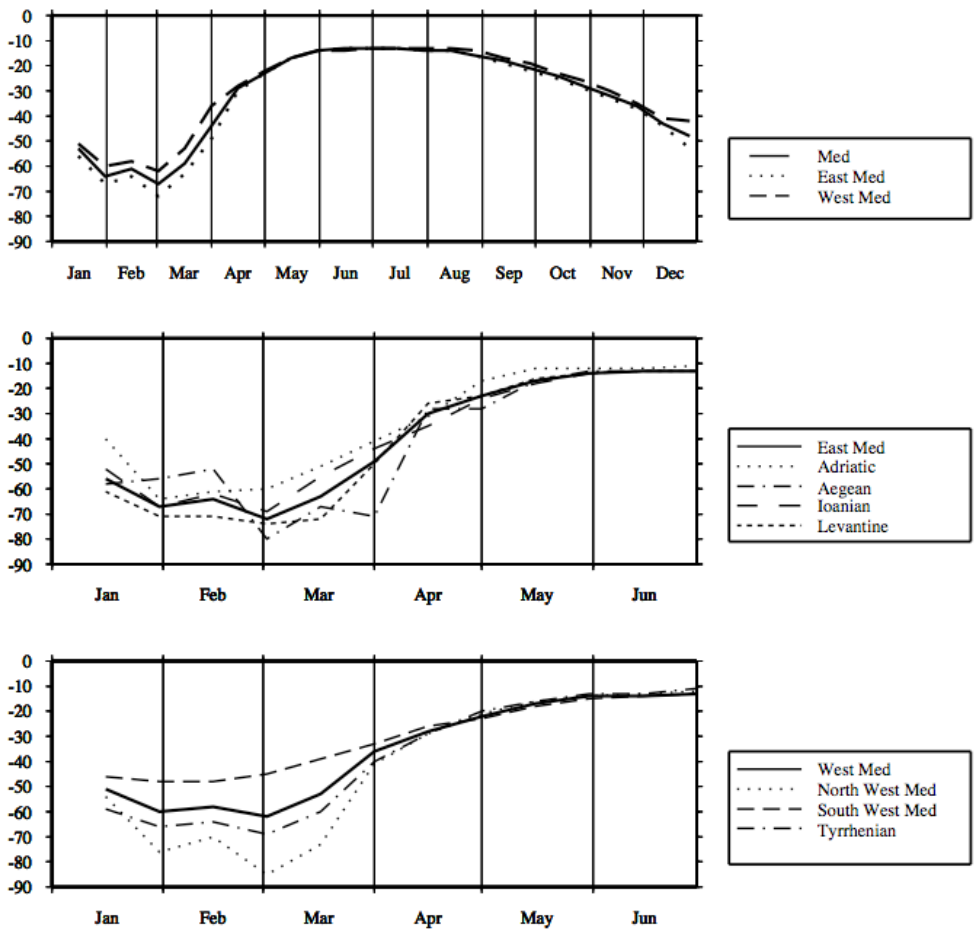


Figure 4. Mixed layer depth time series averaged on different Mediterranean regions (see legends on figures). The two lowest panels show winter and spring climatological evolution detailed into basins and sub-basins.

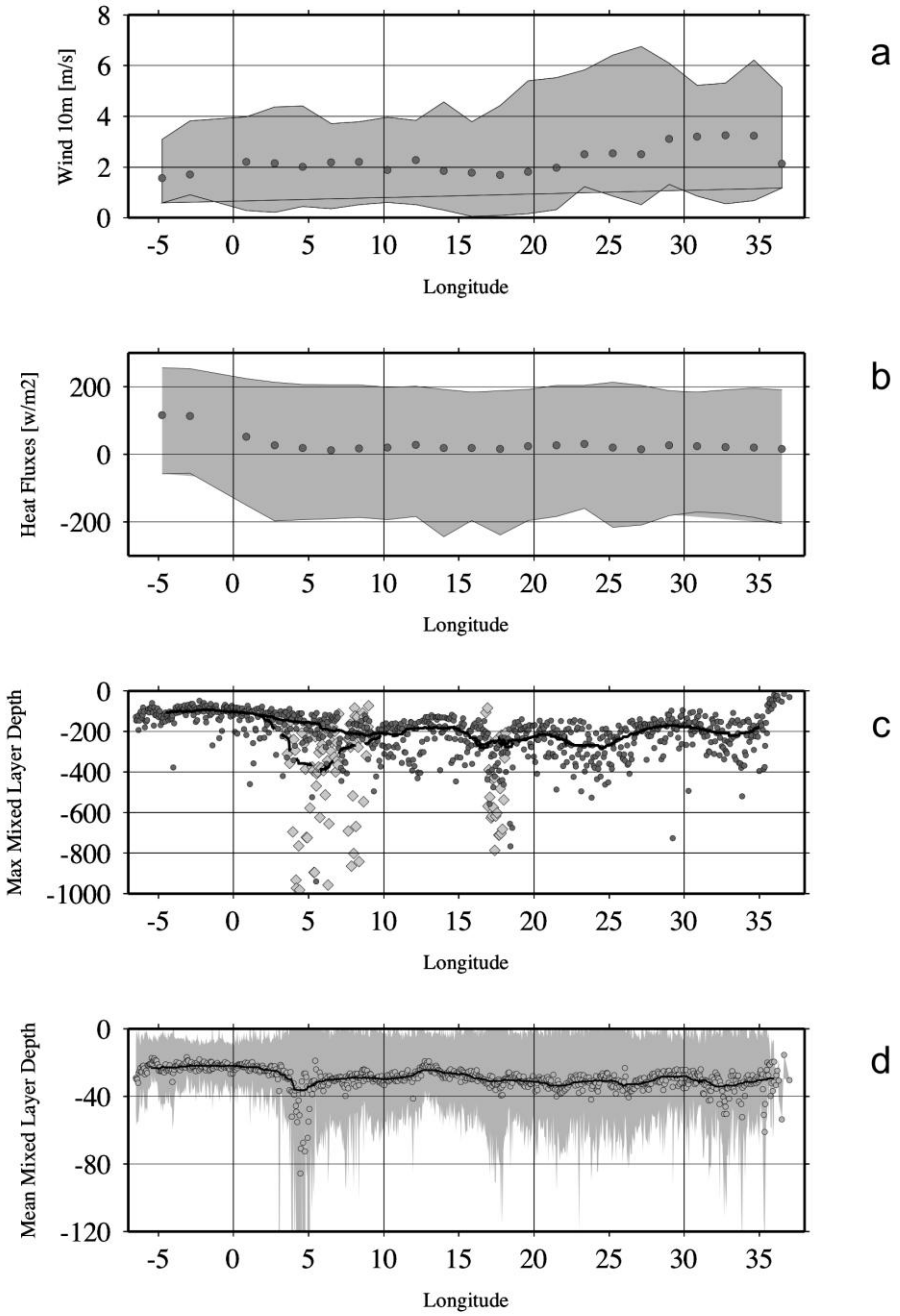


Figure 5. Panels a and b: NCEP climatological fields, respectively of the mean annual winds and heat fluxes, averaged on 0.1° longitudinal belts (grey lines indicate standard deviations). Panel c: maxima values for each 0.1° latitudinal belt (dark grey circles); grey diamonds indicate Gulf of Lions and the Southern Adriatic values; black and grey lines indicate a 5° running average with and without Gulf of Lions and Southern Adriatic observations, respectively. Panel d: latitudinal averages at 0.1° resolution of climatological mixed layer depths (open circles, black line indicates a 5° running average) and standard deviations (grey lines). Mixed layer observations were extracted from the D'Ortenzio et al. (2005) database.

Given this general pattern, however, the timing of the maxima (central and lower panels, zoomed on winter months) is different in the considered sub-basins, spanning from late January for the South WMED to late March for the Aegean Sea. Moreover, the mean winter mixed layer depth is slightly deeper in the EMED than in the WMED (Figure 4, upper panel). Maxima values for the EMED are observed in the Levantine area, (70 m during winter, Figure 4, central panel), which are generally deeper than the mean WMED mixed layer depths. However, in the western area (Figure 4, lower panel) and in particular in the northwestern region, mean values of about 90 m are observed.

To elucidate this point, latitudinal averages (at 0.1° resolution) were calculated from the mixed layer depth climatological field of D'Ortenzio et al. (2005). Maxima values for each 0.1° latitudinal belt were also extracted (Figure 5, panels c and d). Similarly, NCEP climatological fields (Klister et al. 2001) of the mean annual winds and heat fluxes on the Mediterranean area were averaged on 0.1° longitudinal belts (Figure 5, panels a and b).

Generally, mixed layer depth values increase eastwards (black lines in panels c and d), although at 4-5°E and at 18-19°E very deep values are observed. They correspond to the areas where dense water formation events are recurrently observed: the Gulf of Lions and the Southern Adriatic. When these regions are considered, the latitudinal averaged mixed layer depth is 271 m for WMED and 245m for EMED (calculated averaging for all the observations in the WMED and EMED regions). However, if the Gulf of Lions and the Southern Adriatic regions are removed from the computation (grey diamonds on Figure 5), values change to 178m and 236m for the WMED and EMED, respectively.

As expected (Figure 5, panel b, but see also Figure 2), climatologic heat flux longitudinal variability (proxy of $J_m$) is not particularly strong, showing small differences between EMED and WMED. Similarly, mean wind values (panel a, Figure 5) are relatively constant in the two sub-basins, although variability is higher in the EMED, as indicated by the important dispersion of the standard deviation curves. However, the effect of high frequency forcing (typical of the wind stress) on EMED mixed layer depths is evident also in standard deviation latitudinal averaging (grey zone in panel d, Figure 5).

It is therefore clear that important deviations in $h$ from the general atmosphere-driven seasonal pattern were observed in the Mediterranean. As spatial analysis should be informative, mean mixed layer depth maps for winter and spring months were generated (Figure 6), as well as standard deviation maps for two winter months (Figure 7), from the D'Ortenzio et al. (2005) data base. Finally, the annual absolute maximum values comprised in the mixed layer database were computed for each mesh box (Figure 8).

1) In the southwestern area of the basin and throughout the Sicily Channel and the Western Ionian Sea, winter mixed layer depths are very shallow (less than 40 m, Figure 6, January/February/March). The observed pattern corresponds to the zone influenced by AW spreading, where the strong halocline limits the response of the upper layers to the atmospheric forcing (see paragraph 3.4). Moreover, low standard deviation values (Figure 7, and see Figure 5 panel d, region from -5 and 5°E) indicate that mixed layer depths related to AW flow are relatively constant. The AW signature progressively disappears in spring, when atmospheric warming generates very thin mixed layer depths throughout the basin.
2) In the Gulf of Lions, Ligurian, and Adriatic Seas, climatological mixed layer depth maximum values are observed during February and March (Figure 6). In these areas,

all located in the northern half of the basin, dense water formation events were recurrently observed, inducing mixed layer depths greater than 2000 m (Medoc Group 1970). Smoothed by the mesh box average, climatological evaluations, as depicted in Figure 6, are shallower. However, associated standard deviations (Figure 7) show high values, indicating that completely mixed profiles, typical of the dense water formation events, are included in the database. In fact, values greater than 1000 m are observed in the Gulf of Lions area (Figure 8), although, interestingly, deep values are present in the entire Ligurian Sea area, as already noted by Gostan (1968) and, more recently, by Smith et al. (2008). In the Southern Adriatic, where dense water formation events are less frequent than in the Gulf of Lions (see for example Cardin and Gacic, 2003), climatological values are lower.

3) Relatively deep mixed layers are depicted in the Levantine basin (near Cyprus, Crete and Rhodes), where important dynamical features (the Ierapetra and Cyprus eddies and the Rhodes cyclonic gyre) were often observed (Theocharis et al. 1993, Brenner, 1989, Zodiatis et al, 1998, Lascaratos et al. 1993). Local maxima are also obtained in the February/March maps at about 22°E, another region interested by a recurrent dynamical feature (the Pelops eddy, Theocharis et al. 1999). In the Eastern Mediterranean, dynamical structures of medium size (50 – 300 km) were often observed and described (see a recent review of Hamad et al. 2008, but also Malanotte Rizzoli et al. 1997). The underlying dynamical mechanisms generating the EMED surface circulation are still not totally clarified (see, for example, the different schema presented by Hamad et al. 2005 and by Robinson et al. 2001). In our context, this point is relatively unimportant. What is certain is that currents, gyres, eddies, jets and fronts (i.e. the sub-basin scale circulation structures) contribute to modify the mixed layer depth field of the Mediterranean, particularly in the EMED. The climatological view allows only partial highlighting of these effects, though they are evident in some areas (Cyprus, Ierapetra, Pelops). Moreover, the high standard deviation values during winter in these regions indicate the fluctuating nature of surface dynamical structures.

In summary, outside some hot spots related to specific conditions, the Mediterranean seasonal mixed layer depth follows classical temperate sea dynamics, prevalently driven by atmospheric forcing. Climatologically, heat fluxes show a weak, but relevant, east-west gradient (see Castellari et al. 1998 and Ruiz et al. 2008), which, however, only partially explains the difference observed in the mixed layer field between EMED and WMED. Our analysis shows that these differences are likely ascribed to wind stress and to AW spreading in the Mediterranean. The AW flow generates a near-surface barrier, particularly strong in the WMED, which is considerably more difficult to mix. The wind mechanically mixes the upper layers and then deepens the mixed layer depth of the eastern areas more efficiently. Moreover, the interaction of the wind forcing with orography could explain the existence of an intense mesoscale activity in the eastern Mediterranean regions, which, in turn, generates local mixed layer depth variations (e.g. Horton et al. 1994). In other words, atmospheric forcing plays a double role in the definition of the Mediterranean mixed layer field. On one hand, it produces the main seasonal patterns, which, as Mediterranean atmospheric forcing is relatively smooth, determine a homogenous temporal evolution of the mixed layer. On the other hand, the high frequency atmospheric forcing (represented by the wind stress and by its

contribution to the heat exchanges at the air-sea interface) induces mixing events, which locally should alter the seasonal pattern.

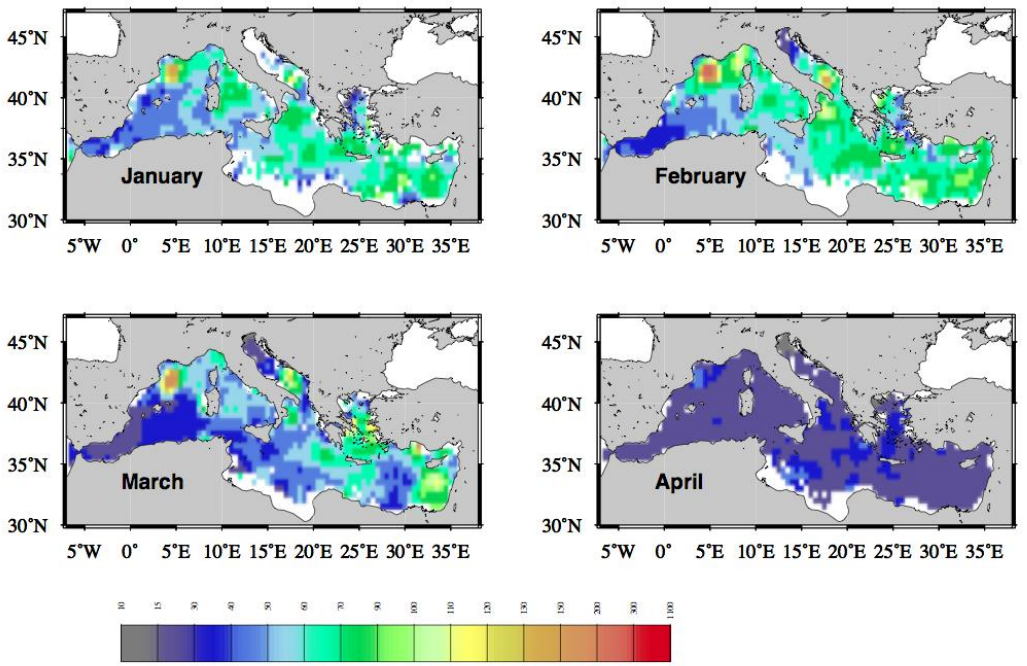


Redrawn from D'Ortenzio et al. 2005.

Figure 6. Mixed layer depth climatology for January, February, March, and April.

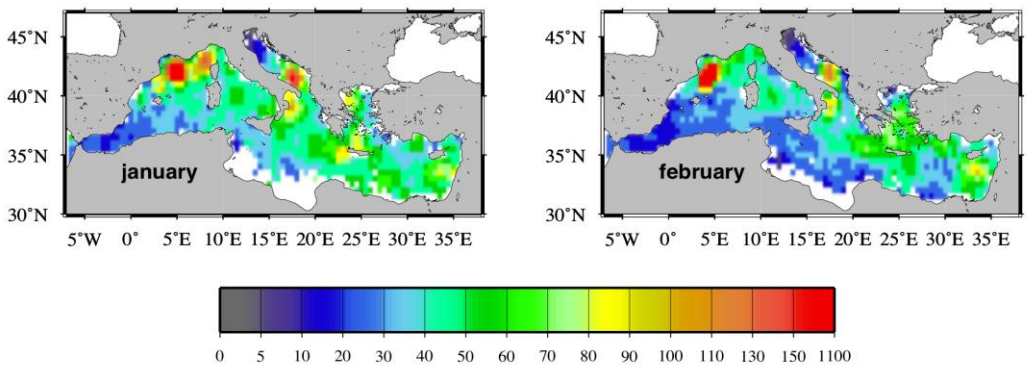


Figure 7. Standard deviation associated to the mesh box averages of the D'Ortenzio et al. (2005) mixed layer climatology for January and February.

In some cases (i.e. dense water formation areas), wind forcing is very localized and, acting together with other processes in a positive feedback, generates very deep mixed layers (i.e. down to ocean bottom). In other cases (i.e. dynamical structures in the Levantine basin), the high frequency of the wind and its interaction with orography produce oceanic dynamical

structures, which locally deepen the mixed layer (forming, for instance Levantine Intermediate waters).

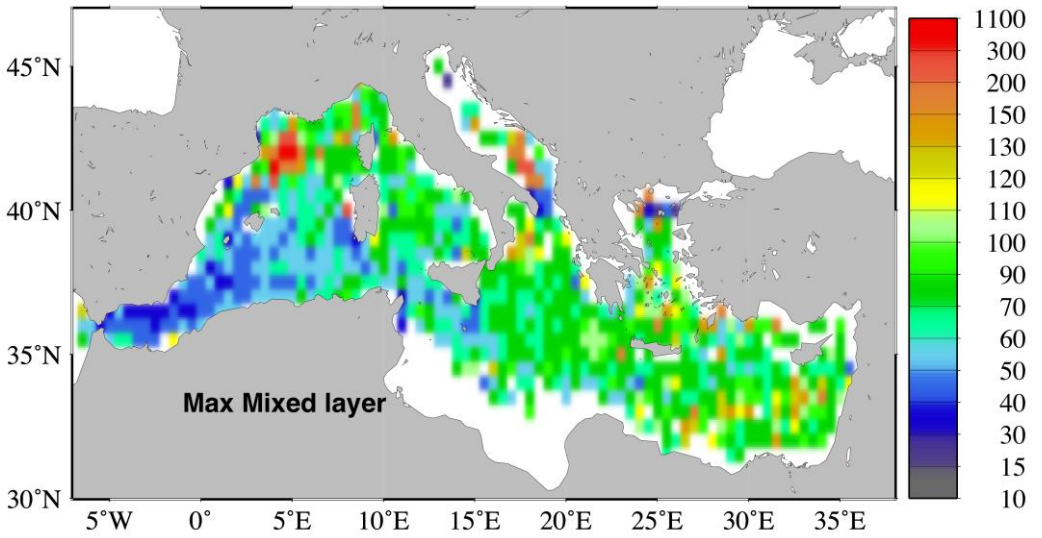


Figure 8. Annual maxima extracted for each mesh box of the D'Ortenzio et al. (2005) mixed layer climatology.

In the next paragraphs, we will try characterize the role of small scale forcing, by discussing spatial and temporal scales separately.

## 4.2. The High Frequencies of Mixed Layer Forcing: The Fall-to-Winter 2001-2002 Transition in the NW Mediterranean

To investigate the effect of high frequency atmospheric forcing on mixed layer dynamics in the open Mediterranean Sea, observations obtained at the station DYFAMED/BOUSSOLE (Ligurian Sea, see Marty et al. 2002 and Antoine et al. 2006) were again used as example. Although not perfect, the DYFAMED/BOUSSOLE data (monthly temperature and salinity profiles since 1991, buoy-derived hourly meteorological observations) represent, to our knowledge, the only available high frequency atmospheric data and concurrent water column observations.

Mixed layer depth (Figure 9, panel d), estimated from in situ profiles (using the temperature criteria used for the climatology of D'Ortenzio et al. (2005) but also using a density criterion) were then calculated from DYFAMED/BOUSSOLE observations from late year 2001 to early 2002 (Figure 9). Concurrent *SST* time series (panel a), mass fluxes (panel b) and wind stress (panel c) were also calculated. Mass fluxes were computed using non-radiative (wind, humidity, air, and sea temperature, hourly measured at Ligurian Sea ODAS buoy, www.meteo.shom.fr/real-titme/html/dyfamed.html) and radiative parameters (obtained from satellite METEOSAT data, Caniaux, unpublished). We selected the end of summer 2001 to spring 2002, equinox time, as in this period, under increasing atmospheric cooling, the

upper ocean shifts from a stratified to an unstratified condition. Three distinct phases are identified:

1) from early September to early November 2001; daily averaged mass flux (thick black line, panel b, Figure 9) is close to zero, whereas instantaneous mass flux (grey line) shows an important diurnal variability, induced by the night-to-day transition (negative/positive values during day/night time, with stratifying/destratifyng effect on the upper ocean). The effect on the upper ocean is, however, relatively modest: only slight *SST* fluctuations are observed, with high (19-21°C) and relatively constant values. Mixed layer depth is very shallow (10 m) and relatively warm, indicating a strongly stratified water column.
2) From early November 2001 to mid January 2002; weather conditions change dramatically and mean mass flux is almost permanently negative. *SST* decreases rapidly (to about 13°C), in particular during a succession of severe wind events (>25m/s, wind stress >1 $N/m^2$), which lasted 1-2 days. Surface water cooling, initially induced by positive mass fluxes, is reinforced by mixing and entrainment processes with deeper waters, which is generated by intense wind events. Under strong mass fluxes and wind forcing, mixed layer depth increased: 75 m in December 2001 to about 100 m in the first days of January 2002 and 140 m late January 2002. Although data scarcity prevents a more precise characterization, we supposed that mixed layer deepening was probably not continuous. The high frequency mixed layer depth variability was, however, evident during the period from January 18-21, when several profiles were collected on the site.
3) From mid-January to March 2002, mean mass flux is relatively constant, exhibiting positive values, which induced mixed layer deepening without, however, any marked change in *SST*. During this phase, diurnal variability of instantaneous mass fluxes is once more observed. However, only weak *SST* variations are observed, as only atmospheric cooling forces mixed layer deepening. The only observation available (February 2002) indicates the unstratified condition of the water column.

The shown example indicates, then, that mixed layer depth and *SST* variability are dramatically different in the three phases. However, for phases 1 and 3, the correspondent mean mass fluxes are relatively close, and cannot entirely explain the observed different behaviors. Most of the variability derives from the diurnal variability of $J_m$ and by the different state of the water column.

In the first phase, the recurrent mixing events occurring during the night, although relevant, are not intense enough to modify the stratification of the water column, which, at the beginning of autumn, is still high. Consequently, the mixed layer depth remains shallow. In contrast, during the third phase, the upper layer is strongly mixed and even the weak warming induced by the day-to-night transition could generate a short duration near-surface shallow layer. The second phase is very different, as mixing intensity hides any impact of the high frequency mass flux variability on mixed layer dynamics.

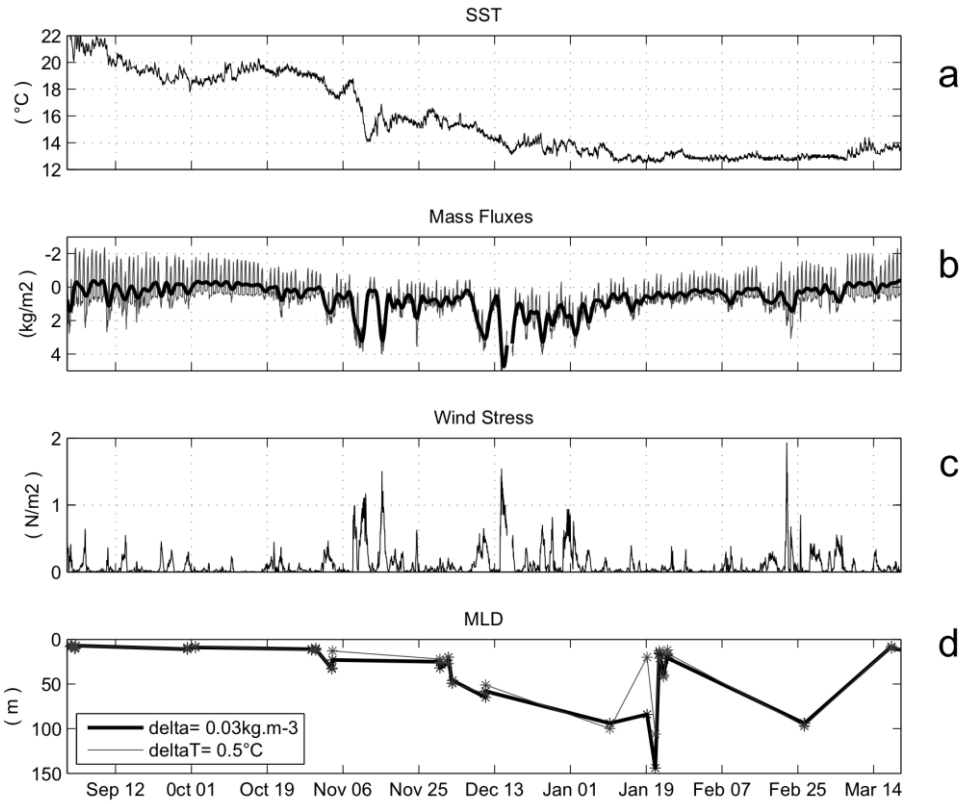


Figure 9. DYFAMED/BOUSSOLE (Ligurian Sea) autumn 2001 to late winter 2002 time series of SST (panel a), mass fluxes (panel b, instantaneous: grey line; daily average black line), wind stress (panel c), mixed layer depth, computed with two different criteria (panel d, thick line: density criteria; thin line: temperature criteria, see appendix).

Summarizing, the effect of high frequency atmospheric forcing on mixed layer evolution is qualitatively different if the upper ocean is strongly or weakly stratified. This impact could be important and, in some cases, could be the main factor influencing mixed layer depth, as highlighted by the DYFAMED/BOUSSOLE data. Consequently, without a characterization of the high frequency (diurnal, for the mass flux and chaotic for the winds), the understanding of cause-effect mechanisms driving the mixed layer evolution could be compromised.

Another point needs attention. The proposed high frequency example neglected any three-dimensional interactions, as the focus was more on temporal than spatial variability. We will discuss in the following the oceanic three-dimensional process impacting on mixed layer dynamics, once more using observational data as an example.

## 4.3. The Effect of the 3 Dimensional Process: The Ekman Pumping in the NW Mediterranean

We already highlighted the role of the three-dimensional oceanic processes in ruling Mediterranean mixed layer dynamics: the spreading of AW, dense water formation and the

eastern basin gyres. Having a permanent or quasi-permanent nature, these features were visible in our climatological analysis. However, smaller structures, generated e.g. as jet instabilities or by a local storm event, could likely induce significant modification of the upper layers. Numerical exercises stressed the importance of three-dimensional processes in the small scale mixed layer depth modification in the Mediterranean (Petrenko et al. 2005, Mounier et al. 2005). However, observational evidences are scarce, because of the intrinsic limits of data acquisition methods at the required spatial scales (Sammari et al. 1995, Fusco et al. 2003).

One of the rare Mediterranean experiments focused on the interplay between a small scale, wind-induced, oceanic structure, local atmospheric forcing, and mixed layer dynamics was performed during a one-month cruise (DYNAPROC, May 1995, Andersen and Prieur, 2000) around the station DYFAMED/BOUSSOLE. More than 170 temperature and salinity profiles were effectuated in a small area (less than 0.5° size) centered on the DYFAMED/ BOUSSOLE station, at high temporal frequency (about 3h and 12h). Atmospheric parameters were recorded onboard at 3h temporal resolution and interpolated, when missing (for example during port calls), with a local meteorological model (see Andersen and Prieur, 2000 for details). The DYNAPROC cruise data offers us a good example to elucidate the effects of the small 3D processes on Mediterranean mixed layer dynamics.

DYNAPROC data are depicted in Figure 10 as time series extracted on the ship locations of wind speed and *SST* (panels c and a,), mass fluxes (panel b), cumulated atmospheric heat fluxes (continuous line on panel f, as evaluated from the atmospheric records), oceanic upper layer heat content (points on panel f, calculated from in situ profiles), mixed layer depth (panel d) and density isolines (panel e).

In the first period of the cruise (May 1-13), the atmospheric heat flux and the oceanic heat content trends (panel f) have similar evolution, characterized by a continuous increase, induced by progressive atmospheric warming. The two time-series diverge abruptly on May 13, when oceanic heat content started decreasing. The two time series fitted again one week later (May 19), with a similar evolution lasting until the end of the cruise (June 2). The abrupt divergence of the time series occurred in correspondence of the passage of an atmospheric cyclone (see the collapse of the atmospheric pressure in Andersen and Prieur (2000) their Figure 5, panel a), which was associated with an intense wind event (Figure 10, panel c). The atmospheric cyclone also induced a positive wind stress curl (not shown here, but see Andersen and Prieur, 2000, Figure 5). As indicated by Andersen and Prieur : “the thermal event delayed the seasonal heating at the time-series station by more than 15 days”.

The upper layer response (indicated by *SST* and mixed layer depth evolution) is similarly characterized by three phases: a warm and shallow mixed layer before the wind event, a cooling and a deepening during and after the wind burst, and a progressive warming at the end of period.

Again, we observe a strong modification of the mixed layer depth, which is not directly related to the mass flux evolution and only slightly dependent on direct wind forcing. Observations indicate that the anomalous upper layer cooling was not induced by atmospheric mass fluxes, which were still increasing (panel b), neither by the mechanical mixing produced by the wind, as sub-surface layers were not modified during the wind event.

The main process influencing the deepening of mixed layer depth is the uplift of isopycnals, observed a few hours before the passage of the atmospheric perturbation (panel e). Ekman pumping, directly proportional to wind stress curl, induced a divergence on the

density field, thus shoaling deep isopycnals. Moreover, Ekman pumping generated a density vertical advection, which explains the divergence between atmospheric and oceanic heat content. The resulting effect is a moderate deepening and strong cooling of the mixed layer associated with strong stratification increase at the base of the mixed layer. In other terms, Ekman pumping induced a local modification of the oceanic density structure by vertical advection, which, in turn, modified mixed layer dynamics, without any direct mass flux forcing.

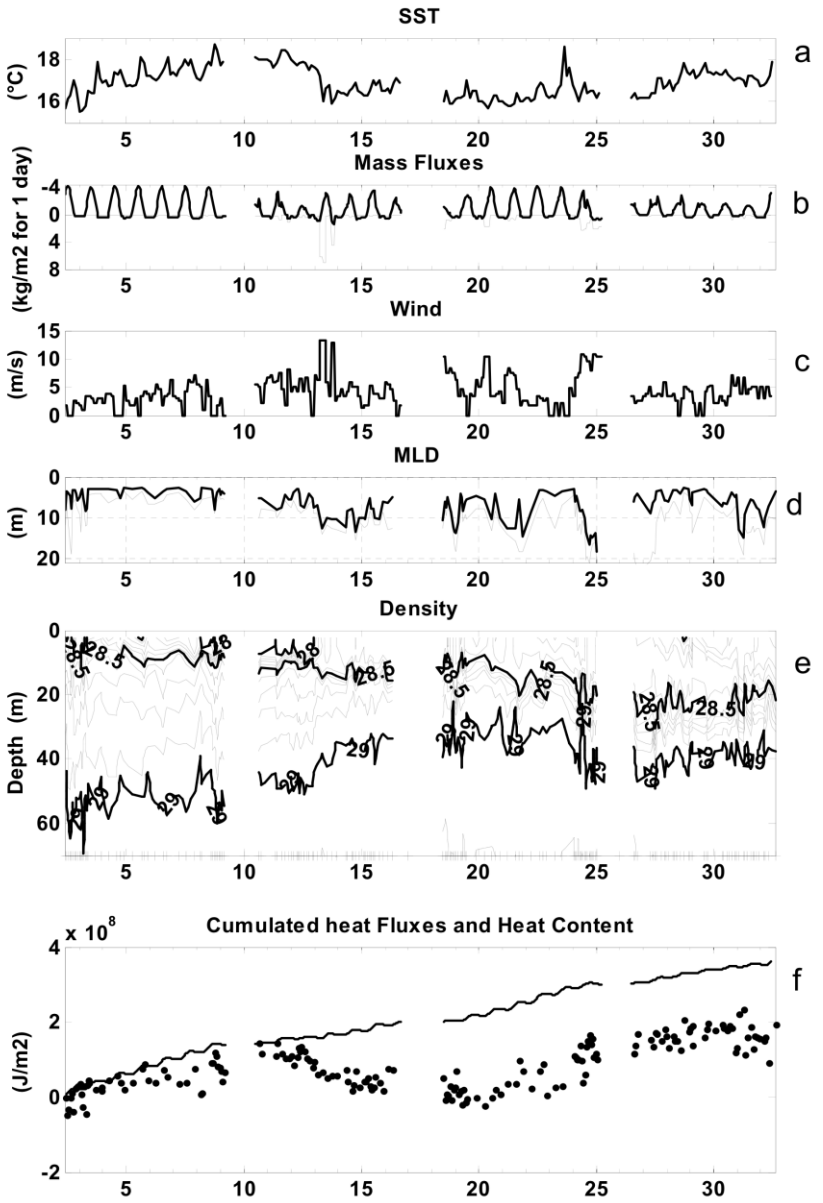


Figure 10. DYNAPROC I cruise time series of SST (panel a,°C), mass fluxes (panel b, kg/m$^2$ for day), wind (panel c, m/s), mixed layer depth (panel d, m), density profiles (panel e), cumulated heat fluxes and upper layer (0-30m) heat content (respectively, lines and dots, panel f). Time axis is in day from May 1, 1995.

The timing of the events (Ekman uplift, wind bursts, heat flux increase), and not only their intensity, was then a key factor to determine local mixed layer dynamics.

## CONCLUSION

To give an overview of Mediterranean Sea upper mixed layer dynamics is not an easy exercise. However, the role of the mixed layer in shaping, controlling, and driving ecological dynamics in the ocean is incontestable. In the Mediterranean, this role is likely more relevant than in other regions of the world's ocean, as the basin's physical circulation and forcing concentrate, in a relatively small area, several and intricate processes.

Although it was already established that the Mediterranean mixed layer follows classical temperate sea dynamics, prevalently driven by the seasonal cycling of atmospheric forcing, other factors could modulate and sometimes strongly modify its evolution. The proximity of the coasts, the complex bathymetry and orography, as well as the hydrological characteristics of surface waters, influenced by the specific thermohaline circulation of the basin, all contribute to complicate our comprehension of the Mediterranean upper ocean mixed layer.

Climatologically, the Mediterranean mixed layer evolution follows a typical temperate sea regime:

1) a progressive mixed layer deepening during fall and winter, forced by atmospheric cooling and the associated mixing;
2) a beginning of stratification in spring, with a consequent creation of a shallow and homogenous surface layer;
3) a permanent and shallow mixed layer in summer, generated by intense warming peculiar of the Mediterranean summer.

This representation, generally common to the entire Mediterranean area, is however complicated by some specific characteristics of the basin, which have a strong impact on mixed layer depth spatial distribution:

1) the AW and its modified elements, which constitute the most widespread surface waters in the basin;
2) dense water formation events in specific areas of the basin, which have a key role in thermohaline cell dynamics but also have a strong impact on mixed layer dynamics;
3) the presence of numerous permanent or quasi-permanent sub-basin gyres and of an intense mesoscale activity;
4) the specific wind regime and its interplay with the complex orography of the Mediterranean coasts.

The resulting mixed layer depth shows important east-west and north-south gradients, hot spots and a high variability (more in the EMED than in the WMED).

Concerning the forcing factors, we have shown, using available observations, that the Mediterranean upper mixed layer dynamics is mainly driven by atmospheric mass flux and

freshwater advection. Additionally, we demonstrated that the former influences mixed layer temporal variability while the latter drives its spatial distribution.

The Mediterranean mass flux field is characterized by four principal temporal scales: interannual, seasonal, diurnal, and chaotic. As the diurnal and the seasonal scales have similar magnitudes, every day the Mediterranean upper ocean undergoes a forcing term that is comparable to the seasonal one. Furthermore, the effect of the mass flux forcing on the water column depends on the state of the water column itself, which explains the different velocity of the stratification/destratification events. Consequently, the resulting mixed layer depth seasonal cycle is de-phased from the mass flux evolution.

Spatially, atmospheric forcing is only weakly variable and thus cannot explain the important differences observed in the Mediterranean mixed layer field. These differences are for the most ascribed to the specific and unique characteristics of the basin surface circulation and, more specifically, by freshwater advection (mainly from the Atlantic, with small though relevant contribution of waters of terrestrial origin). The surface layer, mostly occupied by the fresher waters permanently flowing from Gibraltar into the Mediterranean, "resists" atmospheric destratification forcing in different ways, following the degree of Atlantic water mixing with the underlying Mediterranean waters. In winter, for example, when the rest of WMED is under strong atmospheric forcing, which should induce a deep mixed layer, the area influenced by the Atlantic flow maintains a relatively shallow mixed layer depth.

In conclusion, the combination of mass flux temporal evolution and freshwater Atlantic flow from east to west determines the different behaviors of the EMED and WMED upper ocean Mediterranean mixed layer, as observed on a climatological scale.

Overall, there is the wind, which plays a very specific role on the Mediterranean mixed layer. It affects the mixed layer at each spatio-temporal scale, by combining recurrent regimes, chaotic pulses, direct and indirect effects. We tried to give an overview of this role, by showing examples based on real data and emphasizing how wind-induced processes are, by definition, hardly detectable in a climatological (or mean) description. Wind could trigger stratification/destratification events, altering mixed layer depth when the mass fluxes or the ocean density fields are in a very different state.

The wind also affects mixed layer depth in an indirect way. The oceanic density field responds directly to the wind spatial structure, by generating oceanic structures having permanent or temporary characteristics. As shown by Molcard et al (2002), but see also Malanotte-Rizzoli and Bergamasco, 1989, the specific wind regime of the Mediterranean Sea should play a role in the development of some of the basin-scale permanent gyres (i.e. Gulf of Lions and Ligurian Sea cyclonic gyre, Rhodes anti-cyclonic eddy). Moreover, the wind stress curl contributes to the appearance or disappearance of several sub-basin ocean features (i.e. Tyrrhenian anticyclonic gyre, Ionian cyclonic gyre). At smaller scales (i.e. meso and sub-meso scales), the wind effect is also responsible for local modification of the existing features, inducing, for example, instabilities at the edge of the gyres or on currents. All the above indicates that the mixed layer depth spatial distribution, primarily induced by the mass flux spatial characteristics, could be strongly modified by the wind effect on the spatial density field.

Finally, we try to demonstrate that the Mediterranean mixed layer, although similar in most terms to the global ocean surface layers, is characterized by some unique specificities. In particular, the role of small scales, spatial and temporal, is especially crucial and, for the most, still uncharacterized in the Mediterranean. New observational platforms, such as

profiling floats or gliders, for investigation of small scales are invaluable tools, which should be carefully considered in future experimental strategies.

## 6. APPENDIX : MIXED LAYER DEPTH OPERATIONAL EVALUATION

In most real cases, the mixed layer depth is estimated from in situ profiles. Consequently, several operational evaluations of the mixed layer depth were proposed in the past (see Kara et al. 2000, Thomson and Fine, 2003, Holte and Talley, 2009 for a complete review of the different techniques). It is out of the scope of this paper to evaluate the advantages or limitations of the existing methods. However, a rapid discussion is required, as most of this chapter is based on mixed layer depths obtained by operational methods applied on in situ data. It is also important to highlight that the complexity of the mixed layer processes avoids defining a "perfect" method to evaluate its depth in any situation/condition. In fact, each method is objective-dependent, and a method could be ideal in one situation, though completely inappropriate in another. This point should be always kept in mind, when a method to evaluate mixed layer depth is used.

In the literature, the methods based on a threshold value from surface values were the most widely used. They were based on density and temperature (reference in Thomson and Fine, 2003) or on the changes in density gradient (Lukas and Lindstrom, 1991). This method was largely employed to evaluate single profile mixed layers and to generate climatological fields (Conkright et al. 2002). Generally, the depth where a 0.03 $kg/m^3$ difference from surface density is obtained is considered a proxy of the mixed layer depth. The use of temperature criteria is generally disregarded, when density profiles are available. It was, however, employed when climatology is aimed, as the number of temperature observations is one or two orders of magnitude greater than the number of salinity profiles. Global climatology based on temperature criteria of 0.5°C was proposed by de Boyer Montegut et al. (2004), and a similar method was used to calculate the Mediterranean climatology of D'Ortenzio et al. (2005).

The selection of threshold values and of the reference depth is another key point. High threshold values were selected (0.03 $Kg/m^3$ or 0.5°C) to avoid the identification of the diurnal mixed layer instead of the seasonal mixed layer (see discussion on Kara et al. 2000). Reference depth is generally selected at the surface (Kara et al. 2000) or at 10 m (de Boyer Montegut et al. 2003.

More complex methods were also proposed. Thomson and Fine (2003), for example, reviewed the existing techniques to propose a new method based on the optimal analysis of the density profile linear segments. Their method did not require the definition of a reference depth. Recently, Holte and Talley (2009) developed a new algorithm to evaluate mixed layer depth from ARGO profiling floats in the southern Indian Ocean. Brainerd and Gregg (1995) showed diurnal cycle observations of surface layer microstructures, which allowed separating mixing and mixed layer.

In the following, we sketched some "practical" suggestions to evaluate mixed layer depth from in situ profiles:

1) establish and define the purposes of the mixed layer evaluation (i.e. climatology, diurnal cycle, biological or chemical impact etc.); your way to compute mixed layer depth will depend of this;
2) on the basis of the first point, evaluate the processes that could be neglected;
3) check near surface observations;
4) eliminate density inversions (i.e. greater than 0.01 $kg/m^3$), which indicate unstable conditions of the water column;
5) estimate mixed layer depth using several methods; check the coherence of the different evaluations;
6) if surface atmospheric fluxes are available, verify the coherence between the oceanic heat content and the atmospheric flux evolutions;

The final estimation should be always associated to an error bar, derived by the statistics on the different methods (points 5 and 6).

## ACKNOWLEDGMENT

The MEDAR/MEDATALS, ECMWF, NCEP, DYFAMED, BOUSSOLE, and PROSAT projects are thanked for the easy access to data used in this chapter. The authors are also grateful to Pierre Testor and Daniele Iudicone, for their helpful comments and suggestions. The authors would also like to acknowledge Guy Caniaux, for invaluable help on managing and calculating heat fluxes.

## REFERENCES

Andersen, V., and L. Prieur (2000), One month study in the open NW Mediterranean Sea (DYNAPROC experiment, May 1995): overview of the hydrobiogeochemical structures and effects of wind events, *Deep Sea Research Part I: Oceanographic Research Papers*, *47*, 397-4

Antoine, D., et al. (2006), *BOUSSOLE : a joint CNRS-INSU, ESA, CNES and NASA Ocean Color Calibration And Validation Activity*, 61 pp., NASA Technical memorandum N° 2006 - 214147.

Astraldi, M., et al. (1999), The role of straits and channels in understanding the characteristics of Mediterranean circulation, *Progress In Oceanography*, *44*(1-3), 65-108.

Bethoux, J. P. (1979), Budgets of the Mediterranean Sea. Their dependence on local climate and on characteristics of the Atlantic water, *Oceanologica Acta*, *2*(2), 157-163.

Bethoux, J. P., and B. Gentili (1999), Functioning of the Mediterranean Sea: past and present changes related to freshwater input and climate changes, *Journal of Marine Systems*, *20*, 33-47.

Bèranger, K., et al. (2005), Seasonal variability of water transport through the Straits of Gibraltar, Sicily and Corsica, derived from a high-resolution model of the Mediterranean circulation, *Progress In Oceanography*, *66*(2-4), 341-364.

Brainerd, K. E., and M. C. Gregg (1995), Surface mixed and mixing layer depths, Deep Sea Research Part I: Oceanographic Research Papers, 42(9), 1521-1543.

Brenner, S. (1989), Structure and evolution of warm core eddies in the Eastern Mediterranean Levantine basin, *Journal of Geophysical Research-Oceans*, *94*(C9), 12593-12602.

Caniaux, G., Brut, A., Bourras, D., Giordani, H., Paci, A., Prieur, L., Reverdin, G. (2005). A 1 Year sea surface heat budget in the northeastern Atlantic basin during the POMME experiment: 1. Flux estimates. *J. Geophys.Res.*. 110, doi:10.1029/2004JC002596.

Cardin, V., and M. Gacic (2003), Long-term heat flux variability and winter convection in the Adriatic Sea, *Journal of Geophysical Research-Oceans*, *108*(C9).

Castellari, S., et al. (1998), A model study of air-sea interactions in the Mediterranean Sea, *Journal of Marine Systems [J. Mar. Syst.]*. *18*, 1-3.

Conkright, M. E., et al. (2002), World Ocean Database 2001, Volume 1: Introduction, in NOAA Atlas NESDIS 42, edited by S. Levitus, p. 167, U.S. Government Printing Office, Washington, D.C.

D'Ortenzio, F., et al. (2005), Seasonal variability of the mixed layer depth in the Mediterranean Sea as derived from in situ profiles, *Geophysical Research Letters*, *32*(12).

de Boyer Montégut, C., et al. (2004), Mixed layer depth over the global ocean: An examination of profile data and a profile-based climatology, *Journal of Geophysical Research. C. Oceans*, *109*(C12003).

Demirov, E. K., and N. Pinardi (2007), On the relationship between the water mass pathways and eddy variability in the Western Mediterranean Sea, *Journal of Geophysical Research-Oceans*, *112*(C2).

Fernandez, V., et al. (2005), Mesoscale, seasonal and interannual variability in the Mediterranean Sea using a numerical ocean model, *Progress In Oceanography*, *66*(2-4), 321-340.

Fusco, G., et al. (2003), Variability of mesoscale features in the Mediterranean Sea from XBT data analysis, *Annales Geophysicae*, *21*(1), 21-32.

Gaspar, P., Y. Gregoris, and J. M. Lefèvre, (1990). A simple eddy kinetic Energy model for simulations of the oceanic vertical mixing: Tests at station Papa and long-term upper ocean study site, *J. Geophys Res.*,95, 16,179-16,193.

Gill, A. E. (1982), *Atmosphere-Ocean Dynamics*, 662 pp., Academic Press, New York.

Gostan, J. (1968), Comparaison entre les conditions hydrologiques et climatiques observées dans le Golfe de Gênes pendant les hivers 1962–1963 et 1963–1964, *Cahiers océanographiques*, *29*, 391–416.

Hamad, N., et al. (2005), A new hypothesis about the surface circulation in the eastern basin of the Mediterranean Sea, *Progress in Oceanography*, *66*(2-4), 287-298.

Hamad, N., et al. (2006), The surface circulation in the eastern basin of the Mediterranean Sea, *Scientia Marina*, *70*(3), 457-503.

Holte, J., and L. Talley (2009), A new algorithm for finding mixed layer depths with applications to Argo data and Subantarctic Mode Water formation, J. Atm. Oceanic Tech, 26, 1920-1939.

Hopkins, T. S. (1978), Physical Processes in the Mediterranean basins, in *Estuarine Transport Processes*, edited by B. Kjerfve, pp. 269-310, Univ. South Carolina Press, Columbia, South Carolina.

Hopkins, T. S. (1985), Physics of the Sea, in *Western Mediterranean*, edited by R. Margalef, pp. 100-125, Pergamon Press.

Hopkins, T. S. (1999), The thermohaline forcing of the Gibraltar exchange, *Journal of Marine Systems*, *20*, 1-31.

Horton, C., J. Kerling, G. Athey, J. Schmitz and M. Clifford. – 1994. Airborne expendable bathythermograph surveys of the Eastern Mediterranean. *J. Geophys. Res.,* 99(C5): 9891-9905.

Kara, A. B., et al. (2000), An optimal definition for ocean mixed layer depth, *Journal of Geophysical Research*, *105*(C7), 16803-16821.

Kistler, R., et al. (2001), The NCEP-NCAR 50-year reanalysis: Monthly means CD-ROM and documentation, *Bulletin of the American Meteorological Society*, *82*(2), 247-267.

Korres, G., et al. (2000), The ocean response to low-frequency interannual atmospheric variability in the Mediterranean Sea. Part II: empirical orthogonal functions analysis, *Journal of Climate*, *13*, 732-745.

Lascaratos, A., et al. (1993), A mixed layer study of the formation of Levantine Intermediate water, *Journal of Geophysical Research*, *98*(C8), 14739-14749.

Lionello, P., et al. (2006)a, Cyclones in the Mediterranean Region: Climatology and Effects on the environment, in *Mediterranean Climate Variability*, edited by P. Lionello, et al., p. 126, Elsevier,, Amsterdam.

Lionello, P., et al. (2006)b, The Mediterranean climate: an overview of the main characteristics and issues. , in *Mediterranean Climate Variability*, edited by P. Lionello, et al., p. 126, Elsevier,, Amsterdam.

Longhurst, A. (1995), Seasonal cycles of pelagic production and consumption, *Progress in Oceanography*, *36*, 77-167.

Malanotte-Rizzoli, P., and A. Bergamasco (1989), The general circulation of the Eastern Mediterranean, Part I: the barotropic, wind-driven circulation, *Oceanologica Acta*, *12*(4), 335-351.

Malanotte-Rizzoli, P., and A. Bergamasco (1991), The wind and thermally driven circulation of the eastern Mediterranean Sea. Part II: the Baroclinic case, *Dynamics of Atmospheres and Oceans*, *15*(3-5), 355-419.

Malanotte-Rizzoli, P., et al. (1997), A synthesis of the Ionian Sea hydrography, circulation and water mass pathways during POEM-Phase 1, *Progress in Oceanography [PROG. OCEANOGR.]. 39*(3), 153-204.

Mann, K. H., and J. R. N. Lazier (1996), *Dynamics of Marine Ecosystems: biological-physical interactions in the oceans*, 496 pp., Blackwell Publishing, New York.

Mariotti, A., et al. (2002), The hydrological cycle in the Mediterranean region and implications for the water budget of the Mediterranean Sea, *Journal of Climate*, *15*(13), 1674-1690.

Marshall, J., and F. Schott (1999), Open ocean deep convection: observations, models and theory, *Reviews of Geophysics*, *37*(1), 1-64.

Marty, J. C. (2002), The DYFAMED time-series program (French-JGOFS), *Deep Sea Research*, *49*(11), 1963-1964.

Matsoukas, C., et al. (2005), Seasonal heat budget of the Mediterranean Sea, *Journal of Geophysical Research-Oceans*, *110*(C12).

MEDAR (2002), MEDATLAS/2002 database. Mediterranean and Black Sea database of temperature salinity and bio-chemical parameters. Climatological Atlas., edited, IFREMER edition.

MEDOC Group (1970), Observation of formation of deep water in the Mediterranean Sea, 1969, *Nature*, *227*, 1037-1040.

Millot, C., and I. Taupier-Letage (2005), *Circulation in the Mediterranean Sea*, Springer Verlag ed., 30 pp.

Molcard, A., et al. (2002), Wind driven general circulation of the Mediterranean Sea simulated with a Spectral Element Ocean Model, *Dynamics of Atmospheres and Oceans*, *35*(2), 97-130.

Mounier, F., et al. (2005), Analysis of the mesoscale circulation in the occidental Mediterranean Sea during winter 1999-2000 given by a regional circulation model, *Progress in Oceanography*, *66*(2-4), 251-269.

Niiler, P. P., and E. B. Kraus (1977), One-dimensional models of the upper ocean, in *Modeling and Prediction of the Upper Layers of the Ocean*, edited by E. B. Kraus, pp. 143-172, Pergamon, Oxford.

Pascual, A., et al. (2007), Mesoscale mapping capabilities of multisatellite altimeter missions: First results with real data in the Mediterranean Sea, *Journal of Marine Systems*, *65*(1-4), 190-211.

Petrenko, A., et al. (2005), Circulation in a stratified and wind-forced Gulf of Lions, NW Mediterranean Sea: in situ and modeling data, *Continental Shelf Research*, *25*(1), 7-27.

Pond, S., and G. L. Pickard (1983), *Introductory Dynamical Oceanography 2nd edition*, 329 pp., Pergamon, Oxford.

Rabier, F., et al. (1998), Extended assimilation and forecast experiments with a four-dimensional variational assimilation system, *Quarterly Journal of the Royal Meteorological Society*, *124*(550), 1861-1887.

Ribera d'Alcalà, M., et al. (2003), Nutrient ratios and fluxes hint at overlooked processes in the Mediterranean Sea, *Journal of Geophysical Research*, *108*(C9), 8106.

Riley, G. A. (1946), Factors controlling phytoplankton populations on Georges Bank, *Journal of Marine Research [J. Mar. Res.]. 6*, 54-73.

Robinson, A. R., et al. (2001), *Mediterranean Sea circulation*, 1689-1705 pp., Academic Press, Harcourt Science & Technology, Harcourt Place, 32 Jamestown Road London NW1 7BY UK, [URL http://www.academicpress.com].

Ruiz, S., et al. (2008), Characterization of surface heat fluxes in the Mediterranean Sea from a 44-year high-resolution atmospheric data set, *Global and Planetary Change*, *63*(2-3), 258-274.

Sammari, C., et al. (1995), Aspects of the seasonal and mesoscale variabilities of the Northern Current in the western Mediterranean Sea inferred from the PROLIG-2 and PROS-6 experiments, *Deep-Sea Research Part I-Oceanographic Research Papers*, *42*(6), 893-917.

Sannino, G., et al. (2009), An eddy-permitting model of the Mediterranean Sea with a two-way grid refinement at the Strait of Gibraltar, Ocean Modeling, 30(1), 56-72.

Smith, R. O., et al. (2008), Observations of new western Mediterranean deep water formation using Argo floats 2004-2006, *Ocean Science*, *4*(2), 133-149.

Sverdrup, H. U. (1953), On conditions for the vernal blooming of phytoplankton., *Journal du Conseil International de l' Exploration de la Mer*, *18*, 287-295.

Theocharis, A., et al. (1993), Water masses and circulation in the central region of the Eastern Mediterranean: Eastern Ionian, South Aegean and Northwest Levantine, 1986-1987, *Deep Sea Research Part II: Topical Studies in Oceanography*, *40*(6), 1121-1142.

Theocharis, A., et al. (1999), A synthesis of the circulation and hydrography of the South Aegean Sea and the Straits of the Cretan Arc (March 1994 January 1995), *Progress in Oceanography*, *44*(4), 469-509.

Thomson, R. E., and I. V. Fine (2003), Estimating mixed layer depth from oceanic profile data., J. Atmos. Oceanic Technol., 20, ,319–329.

Tonani, M., et al. (2008), A high-resolution free-surface model of the Mediterranean Sea, *Ocean Science*, *4*(1-4).

Williams, N. (1998), The Mediterranean Beckons to Europe's oceanographers, *Science*, *229*, 463-464.

Williams, R. G., and M. J. Follows (2003), Physical Transport of Nutrients and the Maintenance of Biological Production, in *Ocean Biogeochemistry: The role of the ocean carbon cycle in global change*, edited by M. Fasham, pp. 19-51, Springer.

Woods, J. D., and W. Barkman (1986), The response of Ocean to solar heating: I. The mixed layer, *Quarterly Journal Royal Metereological Society*, *112*, 1-27.

Zecchetto, S., and C. Cappa (2001), The spatial structure of the Mediterranean Sea winds revealed by ERS-1 scatterometer, *International Journal of Remote Sensing*, *22*(1), 45-70.

Zodiatis, G., et al. (1998), Hydrography and circulation south of Cyprus in late summer 1995 and in spring 1996, *Oceanologica Acta*, *21*(3), 447-458.